Journal of Power Sources 182 (2008) 91–94

Contents lists available at ScienceDirect

Journal of Power Sources

journal homepage: www.elsevier.com/locate/jpowsour

Short communication

Carbon-supported Pd nanocatalyst modified by non-metal phosphorus for the oxygen reduction reaction

Lifeng Cheng[a,b], Zhonghua Zhang[a,c], Wenxin Niu[a,c], Guobao Xu[a,*], Liande Zhu[b,**]

[a] State Key Laboratory of Electroanalytical Chemistry, Changchun Institute of Applied Chemistry, Chinese Academy of Sciences, 5625 Renmin Street, Changchun, Jilin 130022, PR China
[b] School of Chemistry, Northeast Normal University, 5268 Renmin Street, Changchun, Jilin 130024, PR China
[c] Graduate University of the Chinese Academy of Sciences, Chinese Academy of Sciences, Beijing 100864, PR China

ARTICLE INFO

Article history:
Received 8 April 2008
Accepted 10 April 2008
Available online 20 April 2008

Keywords:
Catalyst
Fuel cell
Oxygen reduction reaction
Phosphorus
Palladium
Sodium hypophosphite reduction method

ABSTRACT

A carbon-supported palladium catalyst modified by non-metal phosphorus (PdP/C) has been developed as an oxygen reduction catalyst for direct methanol fuel cells. The PdP/C catalyst was prepared by the sodium hypophosphite reduction method. The as-prepared Pd nanoparticles have a narrow size distribution with an average diameter of 2 nm. Energy dispersive X-ray analysis (EDX), X-ray photoelectron spectroscopy (XPS), and X-ray diffraction (XRD) results indicate that P enters into the crystal lattice of Pd and forms an alloy. The PdP/C catalyst has an oxygen reduction reaction (ORR) activity comparable to the commercial Pt/C catalyst and a higher activity than the Pd/C catalyst synthesized by the conventional $NaBH_4$ reduction method. Its high catalytic activity can be attributed to its small size, lower relative crystallinity, and the formation of PdP alloy.

1. Introduction

Proton exchange membrane fuel cells (PEMFCs) and direct methanol fuel cells (DMFCs) are attracting more and more attention as environmentally friendly power sources for transportation and stationary applications. The oxygen reduction reaction (ORR) is a fundamental reaction in fuel cell systems. Platinum has been widely used as the catalyst for the ORR because of its high catalytic activity, but its high price and poor methanol tolerance ability have urged the development of non-platinic materials, such as ruthenium-based materials [1–4], macrocycle catalysts [5–7], and Pd [8–23]. Pd has a similar valence shell electronic configuration and lattice constant to platinum. It is less expensive and relatively abundant compared to Pt. More importantly, the Pd catalyst is highly methanol tolerant [8,9], making it a promising alternative material for the ORR. To further improve its catalytic activity and stability for the ORR, many metallic elements such as Ti [10], Au [11], Co [12–20], Fe [21], Ni [22], etc. were added to Pd. These metallic elements, however, easily leaked into the strong acid electrolyte under electrochemical oxidative conditions. Some non-metals, such as S and Se, were also added to Pd [23], they had little positive effect on the catalytic activity of Pd, and S was even deleterious.

In this paper, we present a new Pd catalyst modified by non-metal phosphorus (denoted as PdP/C) to greatly improve the catalytic activity of Pd for the ORR. The catalyst was prepared by the sodium hypophosphite reduction method. The nature and function of phosphorus in the catalyst were analyzed.

2. Experimental

PdP/C (20 wt.% Pd) catalyst was prepared by the sodium hypophosphite reduction method [24–26]. First, an appropriate amount of $PdCl_2$ aqueous solution was thoroughly mixed with Vulcan XC-72 carbon by sonication and agitation. NaH_2PO_2 solution at a molar ratio of Pd:P = 1:60 was then added into the above mixture. The pH of the solution was adjusted to ca. 9 by a 5% NaOH solution. The solution was heated to 90 °C for 10 h and then cooled in air before the catalyst was filtered and washed with distilled water. Finally the catalyst was dried at 80 °C in a vacuum oven. For comparison, Pd/C (20 wt.% Pd) catalyst was prepared with the conventional impregnation method by reduction of $NaBH_4$.

The TEM images were recorded on a JEOL 2010 transmission electron microscope operating at 200 kV. The composition of the prepared catalysts was estimated by energy dispersive X-ray analysis (EDX) on a JEOL JAX-840 scanning electron

* Corresponding author. Tel.: +86 431 85262747; fax: +86 431 85682747.
** Corresponding author. Tel.: +86 431 85099787; fax: +86 431 85269667.
E-mail addresses: guobaoxu@ciac.jl.cn (G. Xu), zhuliande@yahoo.com.cn (L. Zhu).

0378-7753/$ – see front matter © 2008 Elsevier B.V. All rights reserved.
doi:10.1016/j.jpowsour.2008.04.024

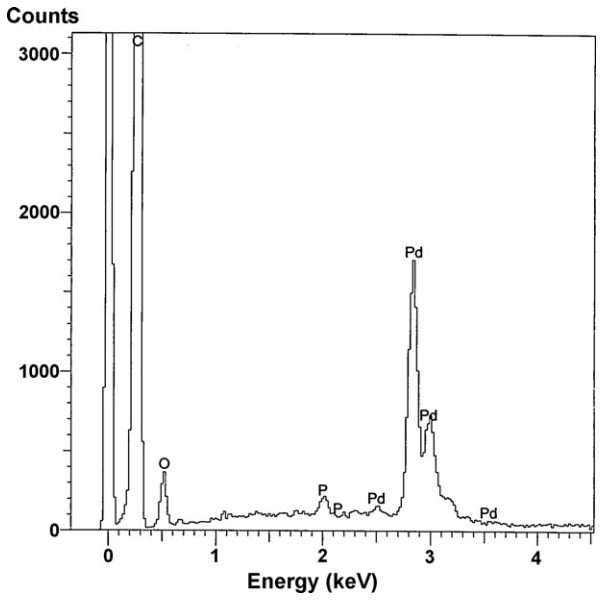

Fig. 1. EDX spectrum of the PdP/C catalyst.

microscope operating at 20 kV. The X-ray diffraction (XRD) patterns for the catalysts were obtained using a Rigaku-D/MAX-PC 2500 X-ray diffractometer with the Cu Kα (λ = 1.5405 Å) radiation source operating at 40 kV and 200 mA. X-ray photoelectron spectroscopy (XPS) measurements were carried out using a Kratos XSAM-800 spectrometer with an Mg Kα radiator. All electrochemical measurements were performed at ambient temperature with an EG&G PARC potentiostat/galvanostat (model 273A) and a conventional three-compartment electrochemical cell. All potentials were referenced to the Ag|AgCl|KCl (sat.) electrode. The working electrode was a rotating glassy carbon electrode (5 mm in diameter) that was covered with the catalysts after being polished and cleaned by sonication. The current density in the electrochemical measurements was normalized to the geometrical surface area of the working electrode.

3. Results and discussion

Fig. 1 shows a typical EDX spectrum of the PdP/C catalyst. The composition of the PdP/C nanocatalyst consists of Pd (17.83 wt.%), P (0.51 wt.%), C (73.29 wt.%), and O (8.37 wt.%). The result indicates that P coexists with the Pd nanoparticles and the atomic ratio of Pd to P is 1.0:0.1. Fig. 2 shows XPS results for the Pd/C and PdP/C catalysts. The binding energies of the C(1s) main peak, Pd($3d_{5/2}$), and Pd($3d_{3/2}$) for the Pd/C catalysts are 284.7 eV, 334.7 eV, and 340.2 eV, respectively. The binding energies of the C(1s) main peak, Pd($3d_{5/2}$), and Pd($3d_{3/2}$) for the PdP/C catalysts are 284.6 eV, 334.8 eV, and 340.4 eV, respectively. A comparison of XPS data between the Pd/C and PdP/C catalysts shows that the shift in the Pd(3d) peak is negligible. Moreover, no signal from P was detectable from the P(2p) spectrum in the PdP/C catalyst [24]. Therefore, P must lie in the interior of the PdP/C nanoparticles. This phenomenon is different from that reported in the literature for PtRuP/C, PtSnP/C, and NiP catalysts [24,25,27].

Fig. 3 displays the XRD patterns of the Pd/C and PdP/C catalysts. In both XRD patterns, the diffraction peak at ca. 25° is due to the (0 0 2) crystal face of carbon. The other diffraction peaks at ca. 39.7°, 45.8°, and 67.8° correspond to the (1 1 1), (2 0 0), and (2 2 0) crystal faces of Pd, respectively. Therefore, the Pd particles in both Pd/C and PdP/C catalysts have a face centered cubic (fcc) structure. The diffraction peaks of the PdP/C catalyst (Fig. 3b) are much broader than those of the Pd/C catalyst (Fig. 3a), showing that the average

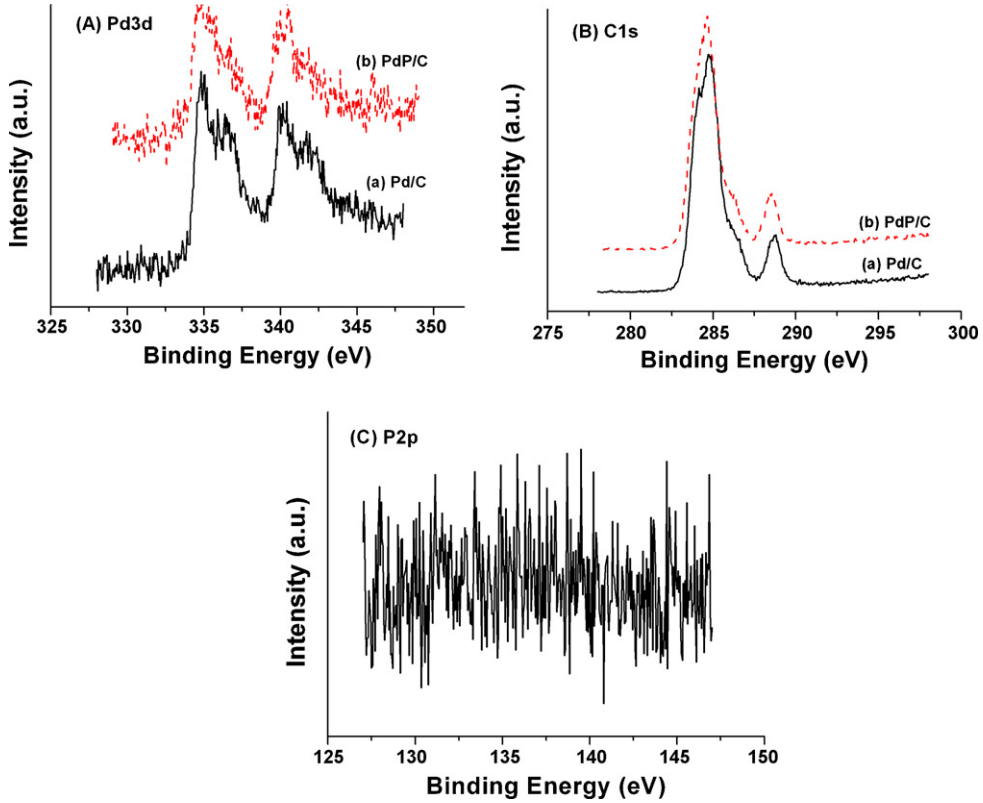

Fig. 2. XPS for the Pd/C and PdP/C catalysts: (A) Pd(3d) spectra, (B) C(1s) spectra, and (C) P(2p) spectrum (only for the PdP/C catalyst).

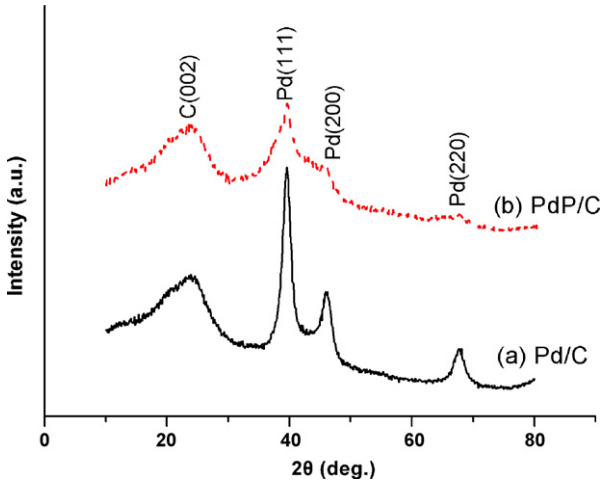

Fig. 3. XRD patterns of the (a) Pd/C and (b) PdP/C catalysts.

size of the Pd particles in the PdP/C catalyst is much smaller than those in the Pd/C catalyst and that the relative crystallinity of the PdP/C particles is much lower than that of the Pd/C catalyst. The average particle size, L, can be estimated from the Pd(2 2 0) peak according to the Scherrer formular [28,29]:

$$L = \frac{0.9\,\lambda_{K\alpha_1}}{B_{(2\theta)}\cos\theta_{max}}$$

where $\lambda_{K\alpha_1}$ is the incident wavelength (1.54056 Å) and $B_{(2\theta)}$ is the width of half peak in radians. The calculated average particle size for the PdP/C and Pd/C catalysts is 2.2 nm and 4.6 nm, respectively. In addition, the 2θ values of the characteristic peaks of the PdP/C catalyst shift towards higher 2θ values compared to those of the Pd/C catalyst. The lattice parameters, a_{fcc}, for Pd particles with fcc structure were evaluated from the angular position of the Pd(2 2 0) peak maxima ($2\theta = 67.86^\circ$ for PdP/C and 67.66° for Pd/C catalysts) according to the following formula [29]:

$$a_{fcc} = \frac{\sqrt{2}\lambda_{K\alpha_1}}{\sin\theta_{max}}.$$

The calculated lattice parameters are 0.3903 nm and 0.3913 nm for the PdP/C catalyst and the Pd/C catalyst, respectively. This indicates that the crystal lattice of Pd contracts in the presence of P. Furthermore, no phosphorus or phosphide phase is observed in the XRD patterns. Therefore, phosphorus has entered into the crystal lattice of Pd at the atomic level.

The TEM images of the Pd/C and PdP/C catalysts are presented in Fig. 4. The nanoparticles in the PdP/C catalyst dispersed more uniformly on the carbon support (Fig. 4a). Moreover, Pd particles in the PdP/C catalyst (Fig. 4b) have smaller sizes and a narrower size distribution than particles in the Pd/C catalyst. The average size of the Pd nanoparticles in the PdP/C catalyst is ca. 2 nm, consistent with the size calculated from the XRD data. The TEM study demonstrates that the addition of phosphorus inhibits the aggregation of Pd particles, leading to higher dispersion of the Pd nanoparticles and a narrow size distribution.

Cyclic voltammograms of the Pd/C and PdP/C electrocatalysts in 0.5 M H_2SO_4 solutions are shown in Fig. 5. The hydrogen adsorption and desorption peaks for both catalysts are located at ca. −0.05 V and 0.05 V, respectively. The area of the hydrogen adsorption and desorption peaks for the PdP/C catalyst (Fig. 5b) are much larger than that for the Pd/C catalyst (Fig. 5a). The Pd oxidation peak of the PdP/C catalyst is located at more negative potential than that of the Pd/C catalyst, indicating that the oxidation of Pd is easier in the presence of P, while the reduction peak of the oxides of the PdP/C catalyst is located at a more positive potential than that of the Pd/C catalyst. This implies that the reduction of the oxides formed during

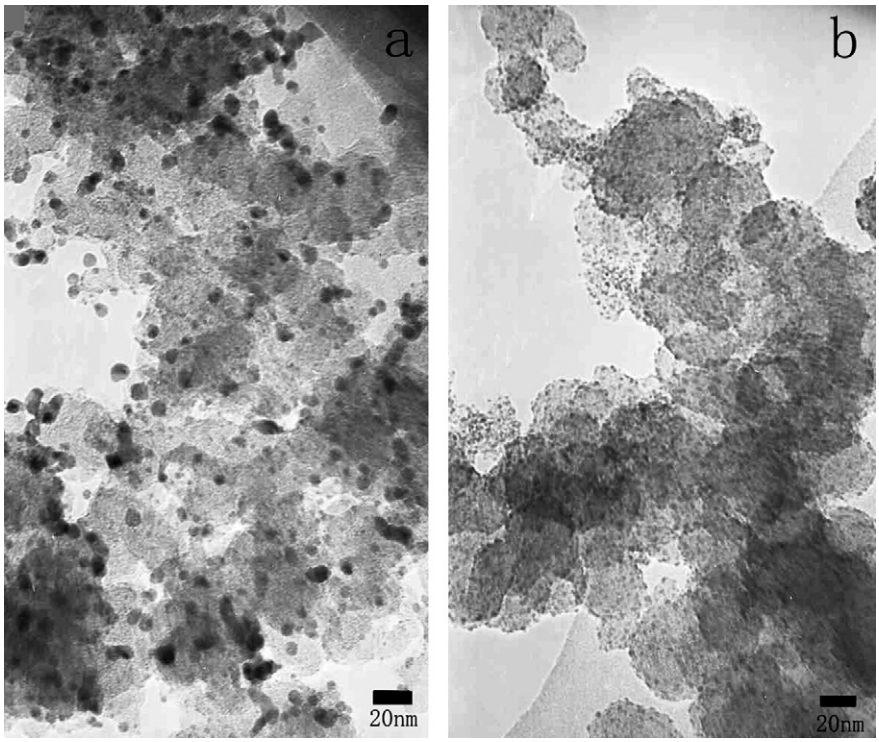

Fig. 4. TEM images of the (a) Pd/C and (b) PdP/C catalysts.

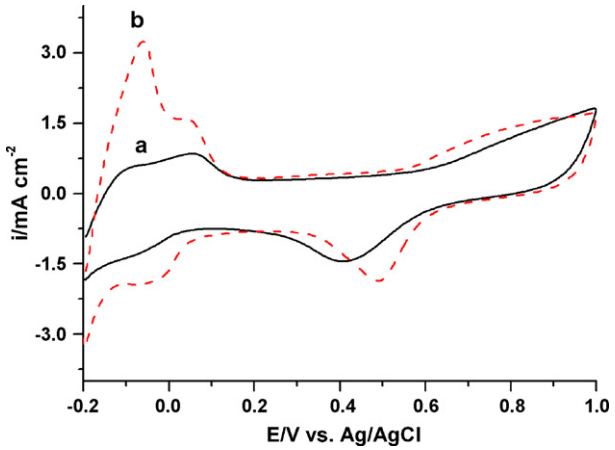

Fig. 5. Cyclic voltammograms of the (a) Pd/C and (b) PdP/C catalysts in 0.5 M H_2SO_4 solutions. Scan rate, 50 mV s^{-1}.

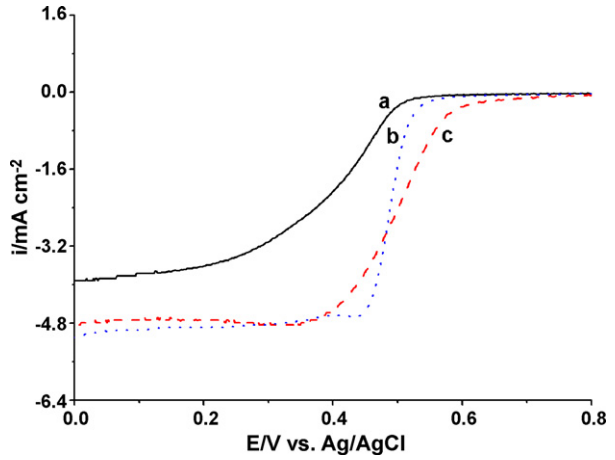

Fig. 6. Linear sweep voltammograms (LSVs) of the (a) Pd/C, (b) PdP/C, and (c) Pt/C (E-TEK) catalyst in 0.5 M oxygen-saturated H_2SO_4 solutions. Sweeping rate, 10 mV s^{-1}; rotation speed, 1500 rpm.

the sweep to positive values is more facile in the presence of P. The shifts in the oxidation peak and reduction peak may be ascribed to the change in nanoparticle size and the formation of the PdP alloy.

Fig. 6 shows linear sweep voltammograms of the Pd/C, PdP/C, and Pt/C (E-TEK) catalysts in 0.5 M oxygen-saturated H_2SO_4 solutions. The onset potential and the half-wave potential for the ORR at the PdP/C catalyst electrode are 50 mV and 85 mV more positive than those at the Pd/C catalyst electrode, respectively. This implies that the PdP/C catalyst is more active than the Pd/C catalyst. The high activity of the PdP/C catalyst can be attributed to smaller nanoparticle sizes, lower relative crystallinity, and formation of the PdP alloy [19,30,31]. The limiting current density at the PdP/C catalyst electrode comes up to the level of the commercial Pt/C (E-TEK 20 wt.%) catalyst and is significantly larger than that of the Pd/C catalyst electrode. The lower limiting current density at the Pd/C catalyst may be ascribed to larger nanoparticle sizes that result in lower Pd surface area.

4. Conclusions

In this study, a PdP/C catalyst was synthesized by the sodium hypophosphite reduction method and exhibited high electrocatalytic activity for the ORR. The physicochemical and electrochemical characterization of the PdP/C catalyst showed that the high electrocatalytic activity of the PdP/C catalyst can be attributed to smaller Pd particle size, lower relative crystallinity, and formation of the PdP alloy. The results demonstrate that the introduction of a non-metal element into Pd catalysts is a promising strategy to develop alternative catalysts for the ORR.

Acknowledgements

This project was supported by the National Natural Science Foundation of China (No. 20505016), the Hundred Talents Program of the Chinese Academy of Sciences, State Key Laboratory of Electroanalytical Chemistry (No. 2006007), and the Department of Sciences & Technology of Jilin Province (20070108).

References

[1] G. Liu, H. Zhang, J. Hu, Electrochem. Commun. 9 (2007) 2643.
[2] C.V. Rao, B. Viswanathan, J. Phys. Chem. C 111 (2007) 16538.
[3] P.K. Babu, A. Lewera, J.H. Chung, R. Hunger, W. Jaegermann, N. Alonso-Vante, A. Wieckowski, E. Oldfield, J. Am. Chem. Soc. 129 (2007) 15140.
[4] A.A. Serov, M. Min, G. Chai, S. Han, S. Kang, C. Kwak, J. Power Sources 175 (2008) 175.
[5] M. Lefevre, J.P. Dodelet, P. Bertrand, J. Phys. Chem. B 104 (2000) 11238.
[6] F. Jaouen, S. Marcotte, J.P. Dodelet, G. Lindbergh, J. Phys. Chem. B 107 (2003) 1376.
[7] N.A. Savastenko, V. Bruser, M. Bruser, K. Anklam, S. Kutschera, H. Steffen, A. Schmuhl, J. Power Sources 165 (2007) 24.
[8] A. Capon, R. Parsons, J. Electroanal. Chem. 44 (1973) 239.
[9] C. Lamy, Electrochim. Acta 29 (1984) 1581.
[10] J.L. Fernandez, V. Raghuveer, A. Manthiram, A.J. Bard, J. Am. Chem. Soc. 127 (2005) 13100.
[11] M. Nie, P.K. Shen, Z. Wei, J. Power Sources 167 (2007) 69.
[12] O. Savadogo, K. Lee, K. Oishi, S. Mitsushima, N. Kamiya, K.I. Ota, Electrochem. Commun. 6 (2004) 105.
[13] V. Raghuveer, A. Manthiram, A.J. Bard, J. Phys. Chem. B 109 (2005) 22909.
[14] M.R. Tarasevich, A.E. Chalykh, V.A. Bogdanovskaya, L.N. Kuznetsova, N.A. Kapustina, B.N. Efremov, M.R. Ehrenburg, L.A. Reznikova, Electrochim. Acta 51 (2006) 4455.
[15] W.E. Mustain, K. Kepler, J. Prakash, Electrochem. Commun. 8 (2006) 406.
[16] W.M. Wang, D. Zheng, C. Du, Z.Q. Zou, X.G. Zhang, B.J. Xia, H. Yang, D.L. Akins, J. Power Sources 167 (2007) 243.
[17] J. Mathiyarasu, K.L.N. Phani, J. Electrochem. Soc. 154 (2007) B1100.
[18] W.E. Mustain, K. Kepler, J. Prakash, Electrochim. Acta 52 (2007) 2102.
[19] L. Zhang, K. Lee, J.J. Zhang, Electrochim. Acta 52 (2007) 3088.
[20] L. Zhang, K. Lee, J. Zhang, Electrochim. Acta 52 (2007) 7964.
[21] M.H. Shao, K. Sasaki, R.R. Adzic, J. Am. Chem. Soc. 128 (2006) 3526.
[22] K. Lee, O. Savadogo, A. Ishihara, S. Mitsushima, N. Kamiya, K.-I. Ota, J. Electrochem. Soc. 153 (2006) A20.
[23] A.A. Serov, S.-Y. Cho, S. Han, M. Min, G. Chai, K.H. Nam, C. Kwak, Electrochem. Commun. 9 (2007) 2041.
[24] X.Z. Xue, J.J. Ge, C.P. Liu, W. Xing, T.H. Lu, Electrochem. Commun. 8 (2006) 1280.
[25] X. Xue, J. Ge, T. Tian, C. Liu, W. Xing, T. Lu, J. Power Sources 172 (2007) 560.
[26] L.L. Zhang, Y.W. Tang, J.C. Bao, T.H. Lu, C. Li, J. Power Sources 162 (2006) 177.
[27] Y. Okamoto, Y. Nitta, T. Imanaka, S. Teranishi, J. Chem. Soc., Faraday Trans 175 (1979) 2027.
[28] E. Antolini, F. Cardellini, J. Alloy Compd. 315 (2001) 118.
[29] V. Radmilovic, H.A. Gasteiger, P.N. Ross, J. Catal. 154 (1995) 98.
[30] Z.H. Zhou, S.L. Wang, W.J. Zhou, G.X. Wang, L.H. Jiang, W.Z. Li, S.Q. Song, J.G. Liu, G.Q. Sun, Q. Xin, Chem. Commun. (2003) 394.
[31] C.P. Liu, X.Z. Xue, T.H. Lu, W. Xing, J. Power Sources 161 (2006) 68.